Jambura Journal of Biomathematics

RESEARCH ARTICLE

Cost-Effectiveness and Optimal Control of Hantavirus Transmission in Rodent Populations

Mahmoud Moustafa[1,✉]

[1]Department of Computer Science, College of Engineering and Information Technology, Onaizah Colleges, Qassim 56447, Saudi Arabia

✉Corresponding author. Email: *mahmoudmoustafa949@gmail.com*

Article Identity
Jambura J. Biomath.
Volume 7 Issue 1 Pages 123 – 135
March 2026, E-ISSN 2723-0317

Article History
Received 21 December 2025
Revised 23 February 2026
Accepted 24 March 2026
Published 27 March 2026

Keywords
Hantavirus, Cost-effectiveness analysis, Optimal control, Numerical simulation

Editorial office: Department of Mathematics, Universitas Negeri Gorontalo, Jln. Prof. Dr. Ing. B. J. Habibie, Bone Bolango 96554, Indonesia

To Cite this Article: Moustafa M. Cost-Effectiveness and Optimal Control of Hantavirus Transmission in Rodent Populations. Jambura Journal of Biomathematics. 2026;7(1):123-135. doi:10.37905/jjbm.v7i1.16

Abstract. *In this paper, we formulate and analyze a deterministic optimal control model for the transmission dynamics of hantavirus infection in rodent populations and identify economically efficient intervention strategies. The model incorporates three time-dependent controls: rodent harvesting, transmission reduction, and alien-oriented control. By applying Pontryagin's Maximum Principle, we derive the Hamiltonian, the adjoint system, and explicit characterizations of the optimal controls, leading to the corresponding optimality system. Numerical solutions are obtained using a forward-backward sweep algorithm. Simulation results demonstrate that combined interventions can substantially reduce the infected rodent population; however, under limited resources, selecting a cost-effective policy is crucial. A health-economic evaluation based on the average and incremental cost-effectiveness ratios (ACER and ICER) shows that the joint implementation of harvesting and transmission reduction provides the most effective strategy among the alternatives considered. We further present a local normalized sensitivity analysis, highlighting the parameters that most strongly influence the predicted infections averted. These findings support the adoption of integrated, rodent-focused interventions for mitigating hantavirus transmission and offer quantitative guidance for informed public health decision-making.*

1. Introduction

Mathematical modeling has become an essential tool for understanding the mechanisms that drive infectious disease transmission and for supporting evidence-based decisions on intervention and resource allocation [1, 2]. In zoonotic infections sustained in wildlife reservoirs, models are particularly valuable because control policies typically target ecological drivers (population density, interspecies interactions, and environmental conditions) in addition to direct transmission pathways. Consequently, a growing body of research has incorporated control policies into biological and epidemiological systems to design, assess, and optimize effective disease-mitigation strategies [3–13]. Hantavirus infection is a prominent example of such systems: it is maintained in rodent populations and can spill over to humans primarily through contact with infected rodents or their contaminated excreta. Consequently, reducing the infection burden often requires integrated management approaches that combine population control, transmission-reduction measures, and ecological interventions that affect the underlying rodent-environment system [14–18].

A number of deterministic compartmental models have been developed to describe hantavirus transmission dynamics in rodent hosts and to investigate key qualitative properties such as threshold behavior and disease persistence [19–21]. However, a systematic cost-effectiveness evaluation of competing integrated control strategies within an optimal-control framework for hantavirus transmission has not yet been examined in detail.

To address this gap, we formulate and analyze an optimal control model for hantavirus transmission in rodent populations that incorporates interactions with an alien species and three time-dependent interventions: (i) rodent harvesting, (ii) transmission reduction, and (iii) alien-oriented control. Using Pontryagin's Maximum Principle, we derive the Hamiltonian, the adjoint system, and explicit characterizations of the optimal controls, leading to the associated optimality system. Numerical solutions are obtained via a forward-backward sweep algorithm. Since public health resources are often limited, we complement the dynamical optimization with a health-economic evaluation by computing the total infections averted, the total control cost, and standard cost-effectiveness measures (ACER and ICER), thereby identifying the most efficient strategy among all feasible combinations of interventions. In addition, we perform a local normalized sensitivity analysis of the effectiveness metric T_a for the most effective strategy (S4), highlighting the parameters that most strongly influence the predicted infections averted.

The remainder of the paper is organized as follows. Section 2 presents the formulation of the hantavirus model and describes the proposed time-dependent control interventions. Section 3 applies Pontryagin's Maximum Principle to derive the Hamiltonian and the characterization of the optimal controls. Section 4 presents the cost-effectiveness analysis and reports the associated numerical simulation results for the proposed control strategies. Finally, Section 5 concludes the paper.

2. Model formulation

We consider the rodent-alien system for hantavirus transmission introduced in [19, 22], in which the total rodent population $r(t) = r_s(t) + r_i(t)$ is divided into susceptible rodents $r_s(t)$ and infected rodents $r_i(t)$, while $z_a(t)$ denotes the population of the alien species. In the original model, the dynamics are governed by

$$\begin{aligned} \frac{dr_s}{dt} &= br - cr_s - \frac{r_s}{k}(r + qz_a) - ar_s r_i - Er_s, \\ \frac{dr_i}{dt} &= -cr_i - \frac{r_i}{k}(r + qz_a) + ar_s r_i - Er_i, \\ \frac{dz_a}{dt} &= (\beta - \gamma) z_a - \frac{z_a}{k}(z_a + \varepsilon r), \end{aligned} \tag{1}$$

where b is the rodent birth rate, c the natural mortality, a the hantavirus transmission rate, E a constant harvesting effort on rodents, q measures the influence of the alien population, k is an environmental parameter, and $\beta, \gamma, \varepsilon$ describe the growth and interaction of the alien species.

To design time-dependent intervention strategies, we introduce three measurable control functions

$$u_1(t),\ u_2(t),\ u_3(t), \qquad 0 \le u_j(t) \le 1,\ j = 1,2,3,$$

with the following biological meanings:

- $u_1(t)$: time-dependent harvesting (or culling) effort applied to the rodent population. This control generalizes the constant rate E in system (1) and represents trapping, poisoning or any removal campaign targeting both susceptible and infected rodents.
- $u_2(t)$: transmission-reduction effort, modeling environmental sanitation, reduction of contact between susceptible and infected rodents, or other measures that decrease the effective hantavirus transmission rate. Mathematically, it reduces the hantavirus transmission from a to $(1 - u_2(t))a$.

- $u_3(t)$: alien-oriented control, such as harvesting of the alien population, habitat modification, or biological control that increases the effective mortality of $z_a(t)$.

Incorporating these controls into system (1), we obtain the controlled system

$$\begin{aligned}
\frac{dr_s}{dt} &= br - cr_s - \frac{r_s}{k}(r+qz_a) - a(1-u_2)r_s r_i - u_1 r_s,\\
\frac{dr_i}{dt} &= -cr_i - \frac{r_i}{k}(r+qz_a) + a(1-u_2)r_s r_i - u_1 r_i,\\
\frac{dz_a}{dt} &= (\beta - \gamma - d\,u_3)z_a - \frac{z_a}{k}(z_a+\varepsilon r),
\end{aligned} \tag{2}$$

where $d>0$ is a scaling parameter that converts the control u_3 into an additional mortality rate for the alien population. The initial conditions are taken as

$$r_s(0) = r_{s0} \geq 0, \quad r_i(0) = r_{i0} \geq 0, \quad z_a(0) = z_{a0} \geq 0.$$

We restrict our attention to bounded, Lebesgue measurable controls:

$$\mathscr{U} = \Big\{(u_1,u_2,u_3) : u_j : [0,T] \to [0,1] \text{ measurable for } j = 1,2,3\Big\}, \tag{3}$$

where $T>0$ denotes the fixed final time of the control horizon. For each triplet $(u_1,u_2,u_3) \in \mathscr{U}$, the controlled system (2) admits a unique positive solution $(r_s(t), r_i(t), z_a(t))$ on $[0,T]$ under the usual Lipschitz and linear-growth conditions.

2.1. Objective functional

The goal of the control program is to reduce the infected rodent population and, where appropriate, to suppress the alien population, while keeping the implementation costs of the controls at a reasonable level. To this end, we consider the quadratic cost functional

$$J(u_1,u_2,u_3) = \int_0^T \left[A_1 r_i(t) + A_2 z_a(t) + \frac{B_1}{2}u_1(t)^2 + \frac{B_2}{2}u_2(t)^2 + \frac{B_3}{2}u_3(t)^2\right] dt, \tag{4}$$

where $A_1, A_2 \geq 0$ weight the epidemiological and ecological burdens associated with infected rodents and alien abundance, respectively, and $B_1, B_2, B_3 > 0$ denote the relative unit costs of the three control measures.

The optimal control problem consists in finding a triplet $(u_1^*, u_2^*, u_3^*) \in \mathscr{U}$ such that the corresponding solution (r_s^*, r_i^*, z_a^*) of system (2) minimizes the objective eq. (4), that is,

$$J(u_1^*, u_2^*, u_3^*) = \min_{(u_1,u_2,u_3)\in\mathscr{U}} J(u_1,u_2,u_3). \tag{5}$$

3. The Hamiltonian and optimality system

This section applies Pontryagin's Maximum Principle to derive the Hamiltonian, the adjoint system, and the explicit characterization of the optimal controls. Let $\lambda = (\lambda_1,\lambda_2,\lambda_3)^\top$ denote the associated costate variables. The Hamiltonian is

$$H = A_1 r_i + A_2 z_a + \frac{B_1(u_1)^2}{2} + \frac{B_2(u_2)^2}{2} + \frac{B_3(u_3)^2}{2} + \lambda_1 \dot{r}_s + \lambda_2 \dot{r}_i + \lambda_3 \dot{z}_a,$$

with $\dot{r}_s, \dot{r}_i, \dot{z}_a$ given by system (2). Pontryagin's Maximum Principle yields $\dot{\lambda}_i = -\frac{\partial H}{\partial x_i}$ and

$$\lambda_1(T) = \lambda_2(T) = \lambda_3(T) = 0.$$

Thus, we obtain

$$\dot{\lambda}_1 = -\lambda_1\left[b-c-\frac{1}{k}(2x_1+x_2+qx_3)-a(1-u_2)x_2-u_1\right]-\lambda_2\left[-\frac{x_2}{k}+a(1-u_2)x_2\right]-\lambda_3\left[-\frac{\varepsilon x_3}{k}\right],$$
$$\dot{\lambda}_2 = -A_1-\lambda_1\left[b-\frac{x_1}{k}-a(1-u_2)x_1\right]-\lambda_2\left[-c-\frac{1}{k}(x_1+2x_2+qx_3)+a(1-u_2)x_1-u_1\right]-\lambda_3\left[-\frac{\varepsilon x_3}{k}\right],$$
$$\dot{\lambda}_3 = -A_2-\lambda_1\left[-\frac{qx_1}{k}\right]-\lambda_2\left[-\frac{qx_2}{k}\right]-\lambda_3\left[(\beta-\gamma)-\frac{1}{k}(2x_3+\varepsilon(x_1+x_2))-du_3\right].$$

3.1. Characterization of the optimal controls

By Pontryagin's Maximum Principle, the optimal controls $u_1^*(t)$, $u_2^*(t)$ and $u_3^*(t)$ minimize the Hamiltonian H pointwise on $[0,T]$. Since H is strictly convex in each control, the optimal controls are obtained by setting $\partial H/\partial u_j = 0$ and projecting the result onto the admissible interval $[0,1]$. The control u_1 appears in H through the quadratic cost $\frac{B_1}{2}u_1^2$ and the removal terms $-u_1 r_s$ and $-u_1 r_i$. The interior minimizer is

$$u_1^{\mathrm{c}}(t) = \frac{\lambda_1(t)r_s(t)+\lambda_2(t)r_i(t)}{B_1}.$$

After projection onto $[0,1]$ we obtain

$$u_1^*(t) = \min\left\{1,\ \max\left\{0,\ \tfrac{\lambda_1(t)r_s(t)+\lambda_2(t)r_i(t)}{B_1}\right\}\right\}.$$

The control u_2 modifies the infection term $a(1-u_2)r_s r_i$. Differentiating the Hamiltonian with respect to u_2 yields

$$u_2^{\mathrm{c}}(t) = \frac{a\,r_s(t)r_i(t)}{B_2}\left(\lambda_2(t)-\lambda_1(t)\right).$$

Thus the optimal control is

$$u_2^*(t) = \min\left\{1,\ \max\left\{0,\ \tfrac{a\,r_s(t)r_i(t)}{B_2}\left(\lambda_2(t)-\lambda_1(t)\right)\right\}\right\}.$$

The control u_3 appears in the alien mortality term $-du_3 z_a$. The unconstrained minimizer satisfies

$$u_3^{\mathrm{c}}(t) = \frac{d\lambda_3(t)z_a(t)}{B_3}.$$

Therefore,

$$u_3^*(t) = \min\left\{1,\ \max\left\{0,\ \tfrac{d\lambda_3(t)z_a(t)}{B_3}\right\}\right\}.$$

These expressions characterize the unique optimal controls associated with the solution of the forward state system and backward adjoint system.

4. Cost-effectiveness and numerical simulations

Before conducting the cost-effectiveness analysis, we summarize the seven control strategies considered in this study in Table 1. Each strategy corresponds to a specific combination of the controls (u_1,u_2,u_3), where u_1 represents rodent harvesting, u_2 reduces the transmission rate, and u_3 targets the alien population.

To compare the seven candidate control strategies defined in Table 1, we performed a cost-effectiveness analysis using the total infections averted, the total control cost, and the associated average and incremental cost-effectiveness ratios. For each strategy, the effectiveness was quantified by the total infections averted

$$T_a = \int_0^T r_i^{\mathrm{nc}}(t)\,dt - \int_0^T r_i^{\mathrm{c}}(t)\,dt, \tag{6}$$

Table 1. Definition of the seven control strategies.

Strategy	Active controls
S1	Rodent harvesting only: $u_1(t)$
S2	Transmission reduction only: $u_2(t)$
S3	Alien-oriented control only: $u_3(t)$
S4	Combined harvesting and transmission reduction: (u_1, u_2)
S5	Harvesting and alien control: (u_1, u_3)
S6	Transmission reduction and alien control: (u_2, u_3)
S7	Full combination: (u_1, u_2, u_3).

where $r_i^{\mathrm{nc}}(t)$ denotes the infected rodent population in the absence of control and $r_i^{\mathrm{c}}(t)$ is the corresponding infected population under the given strategy. Thus, $T_a > 0$ indicates that the strategy reduces the cumulative infected-rodent burden relative to the uncontrolled baseline, whereas $T_a < 0$ implies that the strategy increases the cumulative number of infected rodents.

The total implementation cost was computed by integrating only the quadratic control terms in the objective functional,

$$T_c = \int_0^T \left(\frac{B_1}{2} u_1^2(t) + \frac{B_2}{2} u_2^2(t) + \frac{B_3}{2} u_3^2(t) \right) dt. \tag{7}$$

For strategies with $T_a > 0$, the average cost-effectiveness ratio (ACER) was calculated as

$$\mathrm{ACER} = \frac{T_c}{T_a}. \tag{8}$$

Moreover, following the standard incremental procedure, we ordered strategies by increasing effectiveness (increasing T_a) and computed the incremental cost-effectiveness ratio (ICER) sequentially as

$$\mathrm{ICER}_j = \frac{T_c^{(j)} - T_c^{(j-1)}}{T_a^{(j)} - T_a^{(j-1)}}, \qquad j = 2, 3, \ldots, \tag{9}$$

where (j) denotes the jth strategy in the ordered list. A strategy is said to be dominated if there exists another strategy that is at least as effective and no more costly, with strict improvement in at least one of the two criteria [23, 24].

Table 2. Cost-effectiveness results for the seven optimal control strategies, ordered by effectiveness T_a.

Strategy	T_a	T_c	ACER	ICER	Dominated	J_{total}
S3	−205.11	5.3359	–	0.050144	Yes	512.33
S7	107.28	21	0.19575	−0.11066	Yes	215.5
S1	287.14	1.0966	0.0038189	13.883	No	602.04
S5	287.72	9.1834	0.031918	1.0732	Yes	23.451
S6	288.78	10.322	0.035742	−68.391	Yes	23.219
S2	288.87	4.2533	0.014724	−5.2258	Yes	572.65
S4	289.3	2.0248	0.006999	–	No	597.79

The computed cost-effectiveness outcomes are reported in Table 2. Strategy S3 (alien-oriented control only) yields negative effectiveness ($T_a = -205.11$), indicating that targeting the alien population alone increases the cumulative infected-rodent burden relative to no control; hence, S3 is strongly dominated and is not a viable option from a health-economic perspective. Although the full combination strategy S7 achieves a relatively small value of the overall objective functional J_{total}, it does so at the highest implementation cost ($T_c = 21$) and delivers only modest effectiveness ($T_a = 107.28$), resulting in the largest ACER; consequently, S7 is also dominated. Among the remaining candidates,

strategies that include the alien-oriented control tend to incur higher costs with limited additional epidemiological gains and are eliminated by dominance in the (T_a, T_c) plane.

Among strategies with positive effectiveness, S1 (harvesting only) provides substantial benefit ($T_a = 287.14$) at very low cost ($T_c = 1.097$), leading to a small ACER. However, the integrated rodent-focused strategy S4 (combined harvesting and transmission reduction) attains the largest effectiveness ($T_a = 289.30$) with a relatively low cost ($T_c = 2.025$) and consequently a low ACER (≈ 0.007). Importantly, S4 remains non-dominated in the incremental comparison, whereas strategies that include alien-oriented control (S5-S7) incur considerably larger costs with limited additional gains in effectiveness and are therefore eliminated by dominance. Overall, the cost-effectiveness results identify the combined harvesting and transmission-reduction strategy S4 as the most effective option, achieving the largest reduction in the cumulative infected-rodent burden (T_a) at a relatively low implementation cost, while S1 remains the most economical strategy with the smallest ACER.

Next, we present numerical simulations illustrating the impact of the optimal control strategies on hantavirus dynamics. The model is integrated using the classical fourth-order Runge-Kutta method coupled with the forward-backward sweep algorithm to assess the impact of various control combinations. In each iteration of the forward-backward sweep, the state equations are solved forward in time from the given initial conditions; the adjoint equations are then solved backward in time using the transversality conditions; finally, the controls are updated via the characterization, and the procedure is repeated until convergence [25]. The biological parameter values are adopted from [19].

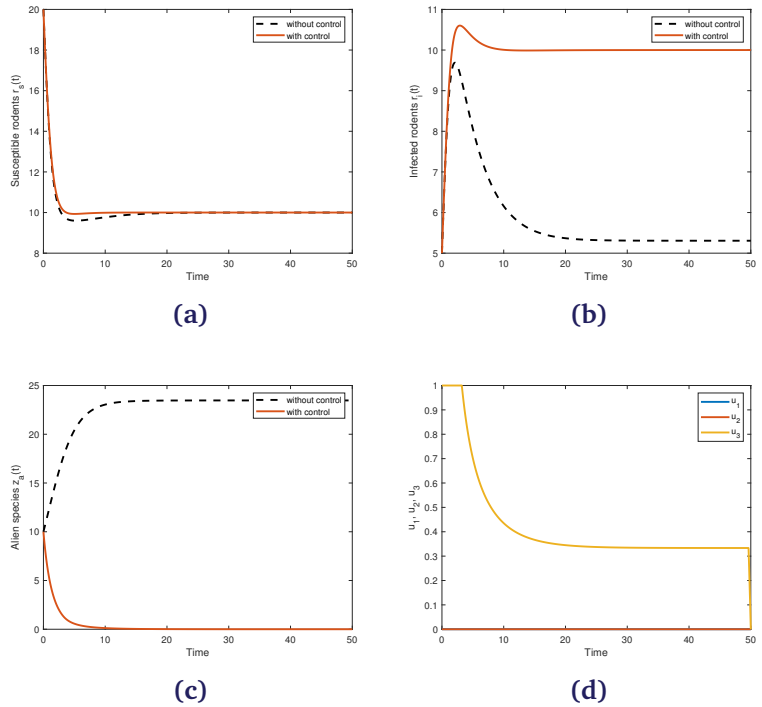

Figure 1. Dynamics of (a) susceptible rodents, (b) infected rodents and (c) alien species when only alien-oriented control is employed; (d) optimal control trajectory.

Figure 1 presents the numerical impact of the alien-only optimal control strategy S3 on the hantavirus dynamics. In this scenario, the control acts exclusively on the alien population, leading to a rapid suppression of $z_a(t)$ relative to the uncontrolled case (Figure 1c), with the corresponding control profile remaining at a relatively high level over an initial time interval before gradually decreasing (Figure 1d). However, despite the substantial reduction in the alien species, the infected rodent pop-

ulation $r_i(t)$ is not mitigated; instead, $r_i(t)$ increases and settles at a markedly higher level compared to the no-control baseline (Figure 1b), while the susceptible rodents exhibit only minor changes (Figure 1a). This behavior is consistent with the cost-effectiveness outcomes, where strategy S3 yields negative effectiveness ($T_a < 0$), indicating an increase in the cumulative infected-rodent burden relative to no control. Consequently, S3 is strongly dominated from a health-economic perspective and should not be regarded as a viable intervention for reducing hantavirus infection.

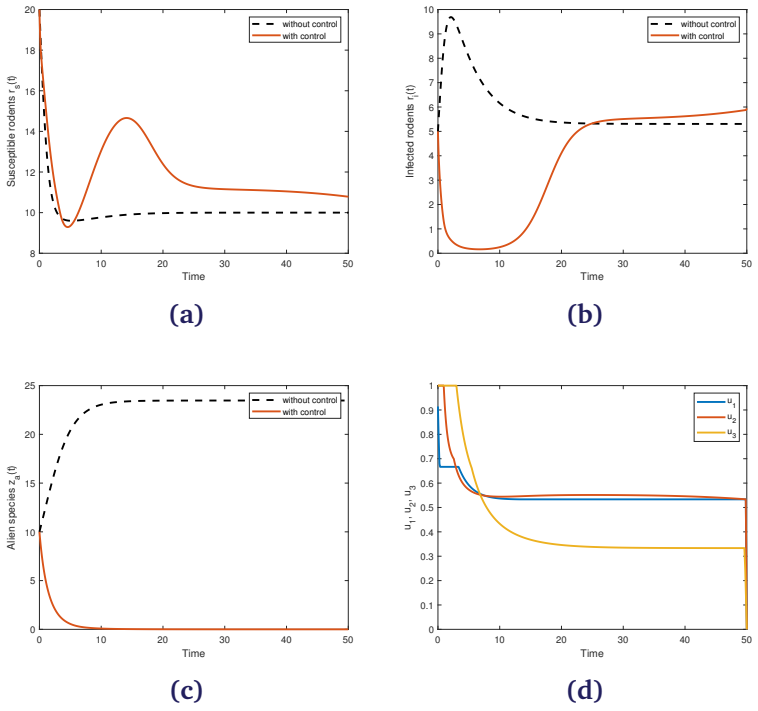

Figure 2. Dynamics of (a) susceptible rodents, (b) infected rodents and (c) alien species when harvesting, transmission reduction and alien-oriented controls are employed; (d) optimal control trajectory.

Figure 2 presents numerical simulations for the full optimal control strategy S7, in which rodent harvesting, transmission reduction, and alien-oriented interventions are implemented simultaneously. As shown in Figure 2c, the inclusion of the alien-oriented control drives the alien population $z_a(t)$ toward near-elimination compared with the uncontrolled case, while the susceptible rodent trajectory exhibits a transient rebound before settling to a level close to the baseline (Figure 2a). In terms of infection dynamics, S7 produces an initial decline in the infected rodents, followed by a gradual increase toward a long-term level comparable to the no-control equilibrium (Figure 2b), indicating that the epidemiological benefit of activating all controls is limited for the infected class under the chosen parameter set. The optimal control profiles (Figure 2d) display the typical pattern of high early effort followed by relaxation, with $u_3(t)$ remaining comparatively larger over time to suppress $z_a(t)$, while $u_1(t)$ and $u_2(t)$ stabilize at intermediate levels.

Figure 3 illustrates the numerical dynamics under the single-intervention strategy S1, where only rodent harvesting is implemented as an optimal control active. Relative to the no-control baseline, harvesting produces a substantial reduction in the infected rodent population $r_i(t)$, driving it toward extinction within a short time window (Figure 3b). As expected, the susceptible class $r_s(t)$ also decreases due to direct removal (Figure 3a). The alien population $z_a(t)$ increases slightly under harvesting (Figure 3c), which can be interpreted as a release of competitive pressure following the

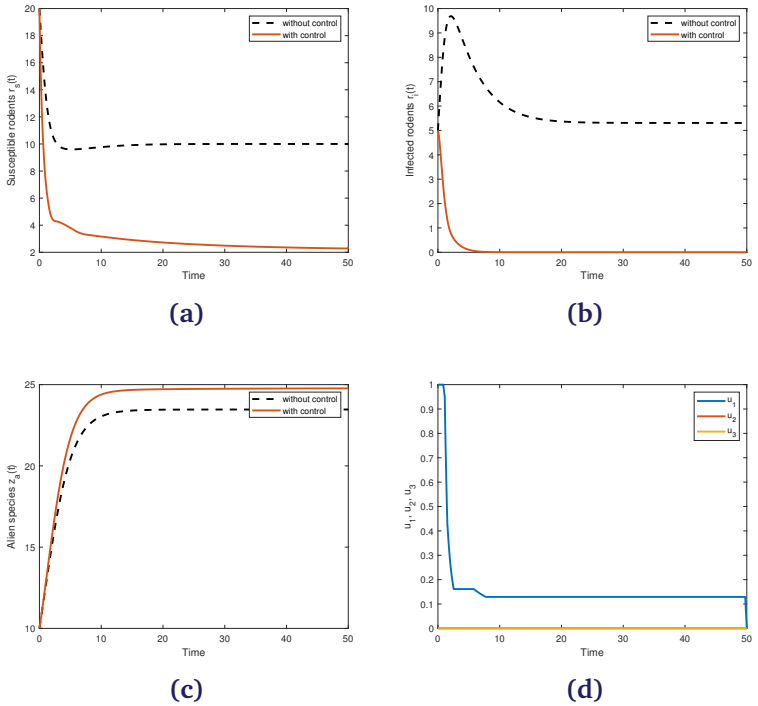

Figure 3. Dynamics of (a) susceptible rodents, (b) infected rodents and (c) alien species when only rodent harvesting control is employed; (d) optimal control trajectory.

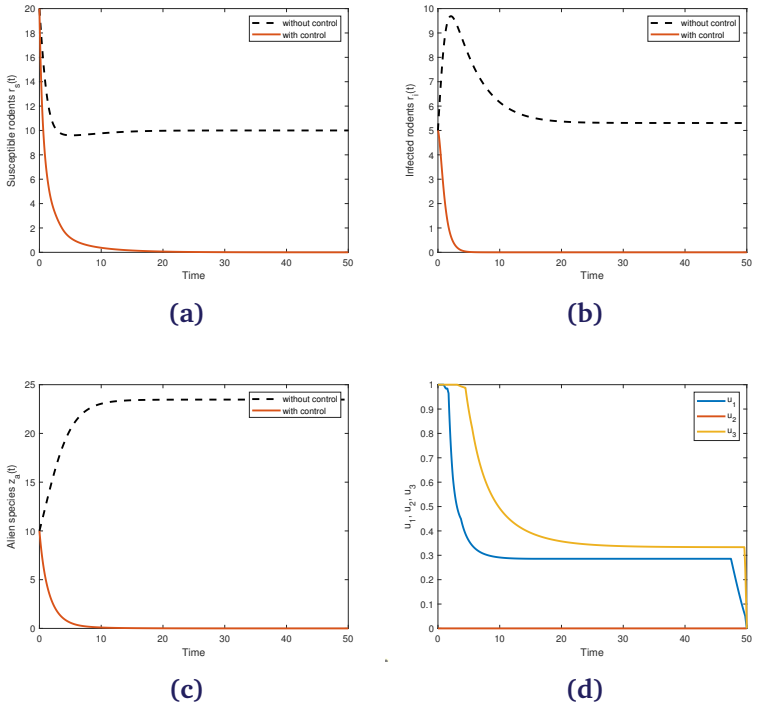

Figure 4. Dynamics of (a) susceptible rodents, (b) infected rodents and (c) alien species when harvesting and alien-oriented controls are employed; (d) optimal control trajectory.

decline in the total rodent population. The optimal harvesting profile in Figure 3d shows that $u_1(t)$ taking relatively high values initially to quickly suppress infection, then relaxing to a lower, nearly steady level as the system approaches the controlled regime.

Figure 4 presents numerical simulations for strategy S5, in which harvesting and alien-oriented control are applied simultaneously. Relative to the uncontrolled dynamics, the combined intervention drives both the susceptible and infected rodent populations toward very low levels (Figures 4a and 4b), reflecting the direct removal effect of harvesting and the resulting reduction in the total rodent population. In addition, activating the alien oriented control yields a pronounced decline of the alien species $z_a(t)$, bringing it close to extinction within a short time interval (Figure 4c). The optimal control profiles in Figure 4d show that $u_1(t)$ starts at a high intensity to quickly suppress the rodent populations and then relaxes to a lower level, whereas $u_3(t)$ remains relatively strong over an initial period to eliminate the alien population before gradually decreasing.

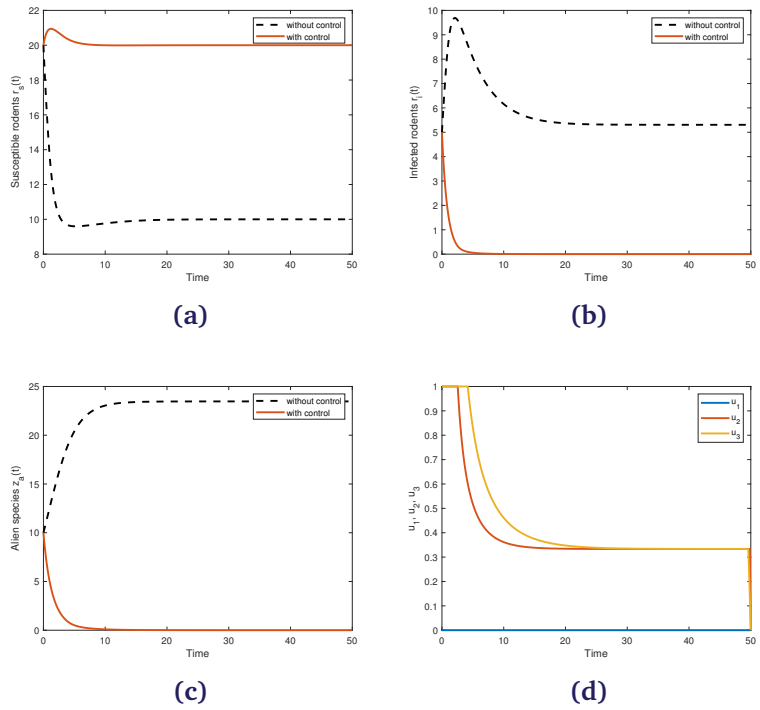

Figure 5. Dynamics of (a) susceptible rodents, (b) infected rodents and (c) alien species when transmission reduction and alien-oriented controls are employed; (d) optimal control trajectory.

Figure 5 shows the numerical dynamics under strategy S6, where transmission reduction and alien-oriented control are implemented simultaneously. Compared with the no-control baseline, the infected rodent population $r_i(t)$ is sharply reduced and approaches extinction (Figure 5b), indicating that reducing the force of infection through u_2 is effective in suppressing hantavirus transmission. In contrast, the susceptible rodent population $r_s(t)$ increases and stabilizes at a higher level than in the uncontrolled case (Figure 5a), which is consistent with the diminished infection pressure and the absence of harvesting. Meanwhile, the alien population $z_a(t)$ is driven down to low levels due to the direct action of u_3 (Figure 5c). The optimal control profiles in Figure 5d show that both $u_2(t)$ and $u_3(t)$ start at relatively high intensities to quickly curtail transmission and suppress the alien species, and then relax to lower levels as the system approaches the controlled regime.

Figure 6 illustrates the numerical dynamics under strategy S2, where only transmission reduction is implemented as an optimal control. Compared with the no-control baseline, the infected rodent

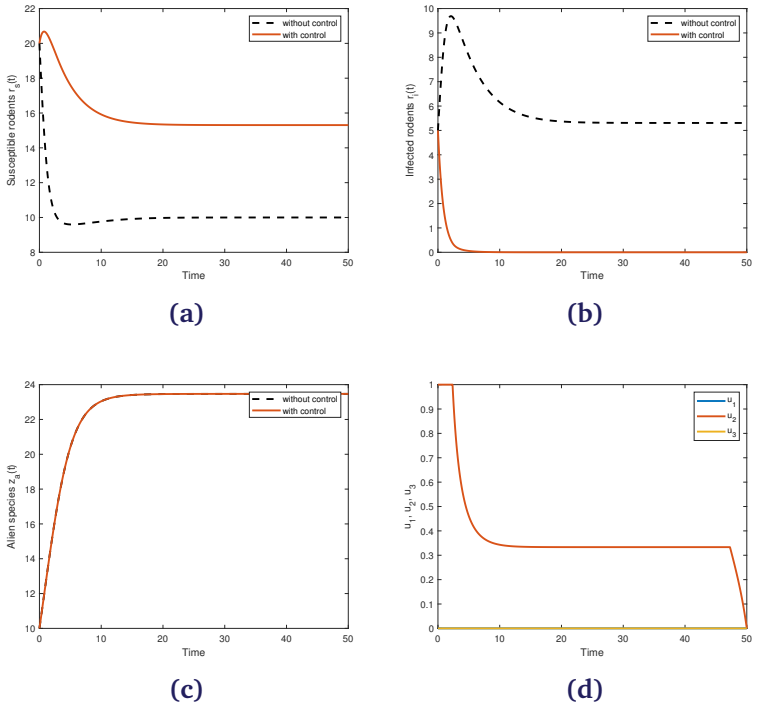

Figure 6. Dynamics of (a) susceptible rodents, (b) infected rodents and (c) alien species when only transmission reduction control is employed; (d) optimal control trajectory.

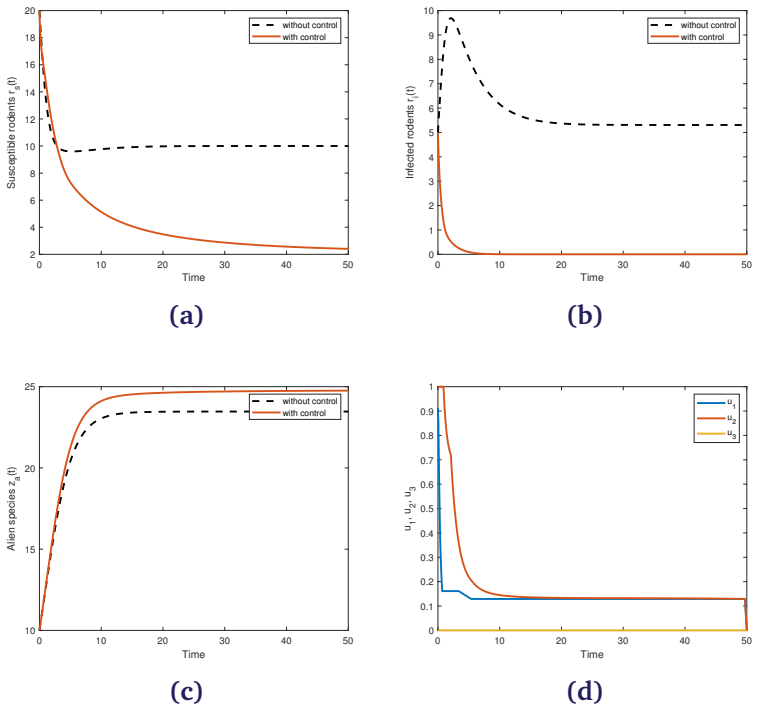

Figure 7. Dynamics of (a) susceptible rodents, (b) infected rodents and (c) alien species when rodent harvesting and transmission reduction controls are employed; (d) optimal control trajectory.

population $r_i(t)$ is reduced and approaches extinction within a short period (Figure 6b), highlighting the effectiveness of reducing the force of infection through u_2. As a consequence of the diminished infection pressure, the susceptible rodent population $r_s(t)$ increases and stabilizes at a higher level than in the uncontrolled case (Figure 6a), reflecting reduced transitions from susceptibility to infection. The alien population $z_a(t)$ remains essentially unchanged relative to the baseline (Figure 6c), since no alien-oriented intervention is applied in this strategy. The corresponding optimal control profile (Figure 6d) shows that $u_2(t)$ taking high values initially to quickly reduce transmission, followed by a gradual decline toward a lower level as the infection burden decreases.

Figure 7 illustrates the dynamical outcomes under the combined rodent harvesting and transmission - reduction strategy. Compared with the no-control baseline, applying the optimal controls substantially suppresses the infected rodent population $r_i(t)$, driving it toward extinction (Figure 7b). This reduction is accompanied by a marked decline in the susceptible rodent population $r_s(t)$ (Figure 7a), reflecting the direct removal effect of harvesting as well as the reduced force of infection induced by transmission mitigation. In contrast, the alien population $z_a(t)$ increases slightly under this strategy (Figure 7c), which can be attributed to the reduced competitive pressure from the rodent population in the coupled system. The optimal control profiles show that $u_1(t)$ and $u_2(t)$ begin at relatively high levels and then decrease smoothly to lower values as the infection burden diminishes, while $u_3(t)$ remains inactive in accordance with the definition of strategy S4. This result is consistent with the cost-effectiveness outcomes, which identify strategy S4 as the most effective intervention among the seven strategies considered.

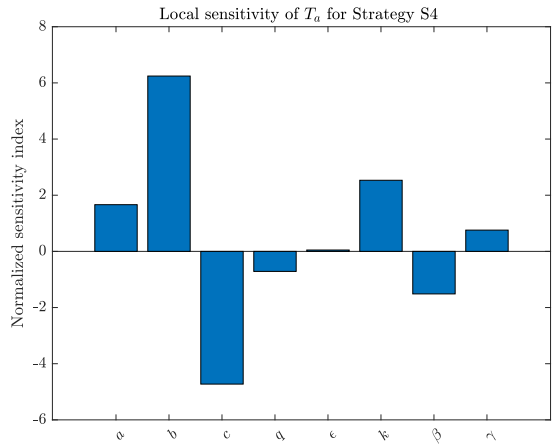

Figure 8. Local normalized sensitivity indices of the effectiveness measure T_a (total infections averted) for strategy S4. Positive (negative) indices indicate that increasing the parameter increases (decreases) T_a.

Figure 8 illustrates the local normalized sensitivity indices of the effectiveness measure T_a (total infections averted) for strategy S4. The figure shows that T_a is most sensitive to the rodent demographic parameters b and c: the rodent birth rate b exerts the largest positive influence (index ≈ 6.2), whereas the natural mortality rate c has a strong negative influence (index ≈ -4.7). This indicates that the predicted effectiveness of strategy S4 depends strongly on rodent recruitment and natural mortality. In addition, the environmental parameter k exhibits a notable positive sensitivity (index ≈ 2.5), and the transmission rate a has a moderate positive effect (index ≈ 1.7). The parameters associated with alien-species dynamics have smaller impacts: β and the alien-influence parameter q show negative sensitivities, while γ has only a minor positive effect and ε is negligible.

5. Conclusion

In this paper, we formulated and analyzed a deterministic model for hantavirus transmission in rodent populations, incorporating an interacting alien species to account for ecological coupling that can influence rodent demography and infection dynamics. The rodent population was partitioned into susceptible rodents $r_s(t)$ and infected rodents $r_i(t)$, while the alien population $z_a(t)$ was included to reflect interspecies interactions within the shared environment.

We then extended the model to an optimal control framework with three time-dependent interventions: rodent harvesting $u_1(t)$, transmission reduction $u_2(t)$, and alien-oriented control $u_3(t)$. By applying Pontryagin's Maximum Principle, we derived the Hamiltonian, the adjoint system, and explicit characterizations of the optimal controls, yielding the complete optimality system. The resulting system was solved numerically via a forward-backward sweep algorithm, enabling a systematic comparison of the epidemiological outcomes across all admissible control combinations.

Numerical simulations show that several integrated strategies can substantially reduce the infected rodent population over the considered time horizon. However, because multi-intervention policies may impose considerable operational costs, we complemented the optimal control analysis with a health-economic evaluation. Specifically, we computed the total infections averted T_a, the total control cost T_c, and the associated cost-effectiveness indicators (ACER and ICER) for each strategy. The results identify strategy S4 as the most effective option, achieving the largest reduction in the cumulative infected-rodent burden (T_a) at a relatively low implementation cost, while S1 remains the most economical strategy with the smallest ACER. In contrast, strategies incorporating alien-oriented control yield only marginal additional epidemiological benefits while substantially increasing costs and are therefore dominated in the cost-effectiveness comparison. Finally, we assessed the robustness of strategy S4 via a local normalized sensitivity analysis of T_a, which indicates that T_a is most sensitive to the rodent demographic parameters b and c, with additional influence from the environmental capacity k and a moderate contribution from the transmission rate a.

Overall, these findings support integrated, rodent-focused interventions as an effective and economically efficient approach for mitigating hantavirus transmission in rodent reservoirs, and they provide quantitative guidance for designing sustainable disease-management policies under limited resources.

Supplementary Information

Author Contributions. **Mahmoud Moustafa:** Conceptualization, methodology, software, validation, formal analysis, investigation, writing—original draft preparation, writing—review and editing, visualization.

Acknowledgements. The authors are thankful the editors and reviewers who have supported us in improving this manuscript.

Funding. This research received no external funding.

Conflict of interest. The authors declare no conflict of interest.

Data availability. Not applicable.

References

[1] Li Y, Xiao Y. Effects of nonlinear impulsive controls and seasonality on hantavirus infection. Mathematical Biosciences. 2025 feb;380:109378. doi:10.1016/j.mbs.2025.109378.

[2] Tessema Alemneh H, et al Makinde. Mathematical Modelling of MSV Pathogen Interaction with Pest Invasion on Maize Plant. Global Journal of Pure and Applied Mathematics. 2019;15(1):55-79.

[3] Peter OJ, Panigoro HS, Ibrahim MA, Otunuga OM, Ayoola TA, Oladapo AO. Analysis and dynamics of measles with control strategies: a mathematical modeling approach. International Journal of Dynamics and Control. 2023 oct;11(5):2538-52. doi:10.1007/s40435-022-01105-1.

[4] Berhe HW. Optimal Control Strategies and Cost-effectiveness Analysis Applied to Real Data of Cholera Outbreak in Ethiopia's Oromia Region. Chaos, Solitons and Fractals. 2020 sep;138:109933. doi:10.1016/j.chaos.2020.109933.

[5] Alqahtani Z, Almuneef A, El-Shahed M. Mathematical Model for the Control of Red Palm Weevil. Axioms. 2024 sep;13(9):637. doi:10.3390/axioms13090637.
[6] Alnafisah Y, El-Shahed M. Optimal control of red palm weevil model incorporating sterile insect technique, mechanical injection, and pheromone traps. Alexandria Engineering Journal. 2024;93:382-91. doi:10.1016/j.aej.2024.02.059.
[7] El-Mesady A, Elsadany AA, Mahdy AMS, Elsonbaty A. Nonlinear dynamics and optimal control strategies of a novel fractional-order lumpy skin disease model. Journal of Computational Science. 2024;79:102286. doi:10.1016/j.jocs.2024.102286.
[8] Oguntolu FA, Peter OJ, Omede BI, Balogun GB, Ajiboye AO, Panigoro HS. Mathematical Modeling on the Transmission Dynamics of Diphtheria with Optimal Control Strategies. Jambura Journal of Biomathematics (JJBM). 2025;6(1):1-22. doi:10.37905/jjbm.v6i1.29716.
[9] Wanjala HM, Okongo MO, Ochwach JO. Mathematical Model of the Impact of Home-Based Care on Contagious Respiratory Illness Under Optimal Conditions. Jambura Journal of Biomathematics (JJBM). 2024;5(2):83-94. doi:10.37905/jjbm.v5i2.27611.
[10] Ludji DG, Hurit RU, Manek SS, Ndii MZ. Comparison of Optimal Control Effect from Fungicides and Pseudomonas Fluorescens on Downy Mildew in Corn. Jambura Journal of Biomathematics (JJBM). 2024;5(1):38-45. doi:10.37905/jjbm.v5i1.23153.
[11] Al Ajlan ZS, El-Shahed M. Mathematical Modeling of the Impact of Desert Dust on Asthma Dynamics. Axioms. 2025;14(8):639. doi:10.3390/axioms14080639.
[12] Afolabi AS, Miswanto M. Mathematical Modeling, Optimal Control and Cost-Effectiveness Analysis of Diphtheria Transmission Dynamics. Jambura Journal of Biomathematics (JJBM). 2025;6(2):88-108. doi:10.37905/jjbm.v6i2.30851.
[13] Jose SA, Raja R, Alzabut J, Rajchakit G, Cao J, Balas VE. Mathematical modeling on transmission and optimal control strategies of corruption dynamics. Nonlinear Dynamics. 2022;109(4):3169-87. doi:10.1007/s11071-022-07581-6.
[14] Alnafisah Y, El-Shahed M. Stochastic Analysis of a Hantavirus Infection Model. Mathematics. 2022;10(20):3756. doi:10.3390/math10203756.
[15] Kocabiyik M, Ongun MY. Distributed order hantavirus model and its nonstandard discretizations and stability analysis. Mathematical Methods in the Applied Sciences. 2025;48(2):2404-20. doi:10.1002/mma.10442.
[16] Moustafa M, Hafiz Mohd M, Izani Ismail A, Aini Abdullah F. Dynamical Analysis of a Fractional-Order Hantavirus Infection Model. International Journal of Nonlinear Sciences and Numerical Simulation. 2020;21(2):171-81. doi:10.1515/ijnsns-2018-0292.
[17] Moustafa M, Abdullah FA, Shafie S, Ismail Z. Dynamical behavior of a fractional-order Hantavirus infection model incorporating harvesting. Alexandria Engineering Journal. 2022;61(12):11301-12. doi:10.1016/j.aej.2022.05.004.
[18] Supriatna AK, Napitupulu H, Ndii MZ, Ghosh B, Kon R. A Mathematical Model for Transmission of Hantavirus among Rodents and Its Effect on the Number of Infected Humans. Computational and Mathematical Methods in Medicine. 2023;2023(1):9578283. doi:10.1155/2023/9578283.
[19] Mohamed Yusof F, Abdullah FA, Md Ismail AI. Modeling and Optimal Control on the Spread of Hantavirus Infection. Mathematics. 2019 dec;7(12):1192. doi:10.3390/math7121192.
[20] Yusof FM, Folarin FM. Modeling the transmission dynamics of Hantavirus infection under the effect of vaccination and other optimal controls. Discovering Mathematics. 2023;45(1):56-75.
[21] Mohamed Yusof F, Md Ismail AI, Abu Hassan AY. Implication of Predator Interaction of the Spread of Hantavirus Infection. Matematika. 2018:205-26. doi:10.11113/matematika.v34.n2.953.
[22] Peixoto ID, Abramson G. The effect of biodiversity on the hantavirus epizootic. Ecology. 2006;87(4):873-9. doi:10.1890/0012-9658(2006)87[873:TEOBOT]2.0.CO;2.
[23] Rodrigues P, Silva CJ, Torres DFM. Cost-Effectiveness Analysis of Optimal Control Measures for Tuberculosis. Bulletin of Mathematical Biology. 2014;76(10):2627-45. doi:10.1007/s11538-014-0028-6.
[24] Berhe HW, Gebremeskel AA, Melese ZT, Al-arydah M, Gebremichael AA. Modeling and global stability analysis of COVID-19 dynamics with optimal control and cost-effectiveness analysis. Partial Differential Equations in Applied Mathematics. 2024;11:100843. doi:10.1016/j.padiff.2024.100843.
[25] Lenhart S, Workman JT. Optimal Control Applied to Biological Models. Chapman and Hall/CRC; 2007. doi:10.1201/9781420011418.